Supplementary Materials

Microstructure and Unusual Ferromagnetism of Epitaxial SnO_2 Films Implanted with Co Ions

Rustam I. Khaibullin [1,2,*], Amir I. Gumarov [1,2], Iskander R. Vakhitov [1,2], Andrei A. Sukhanov [1], Nikolay M. Lyadov [1,2], Airat G. Kiiamov [2], Dilyara M. Kuzina [3], Valery V. Bazarov [1], and Almaz L. Zinnatullin [1,2]

[1] Zavoisky Physical-Technical Institute, FRC Kazan Scientific Centre of RAS, Kazan 420029, Russia
[2] Institute of Physics, Kazan Federal University, Kazan 420008, Russia
[3] Institute of Geology and Petroleum Technologies, Kazan Federal University, Kazan 420008, Russia

* Correspondence: allzinnatullin@kpfu.ru

1. Angular X-ray diffraction study of Co ions implanted SnO_2 films

The θ-2θ XRD scans of both as-prepared and Co-ions implanted SnO_2 films taken at the selected tilt angles (ψ) as well as the orientation dependencies (φ-scans) of XRD reflexes intensities were recorded using Bruker D8 Advance diffractometer, equipped with an X-ray tube with the Cu-Kα anode (λ=0.15418 nm).These XRD measurements are presented in **Figures S1-S3**. From a comparison of the XRD patterns shown in **Figure S1** and **Figure S2(a),** it is clearly seen that Co ions implantation strongly influence on shape of (101) SnO_2 reflections in the case of Co ions implantation at room temperature only, whereas such complexation of the reflexes shape was not observed at the elevated temperature of implantation (**Figure S3(a)**). At the same time there are not any notably broadening of (110) SnO_2 reflexes after Co ion implantation as it seen in **Figures S2(b) and S3(b)**.

The φ-scans show similar six-fold dependencies of XRD reflexes intensity in both as-prepared and Co ions implanted SnO_2 films (see insets in **Figures S1-S3**). The observed six-fold patterns should be related with growth of three equivalent domains of SnO_2 film during the synthesis. The manifestation of the angular dependences of XRD reflexes in the Co implanted samples show that the SnO_2 films preserve their epitaxial nature after ion irradiation.

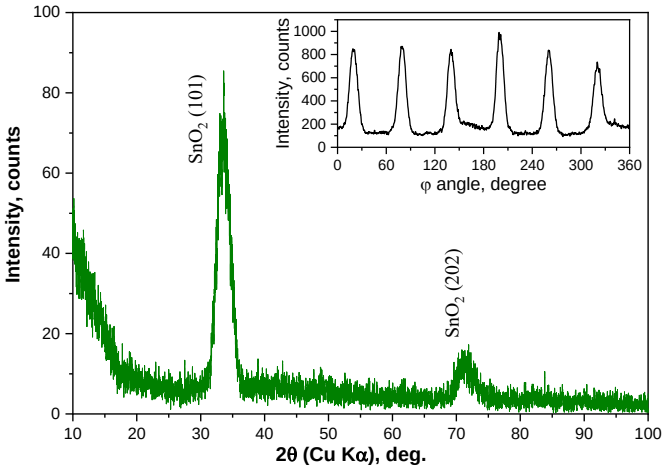

Figure S1. θ-2θ scan of the SnO_2 film before implantation under fixed angles of ψ = 56.2° and φ = 79.9°. The inset shows the φ-scan of the (101) reflex under 2θ = 33.7° and ψ = 56.2°.

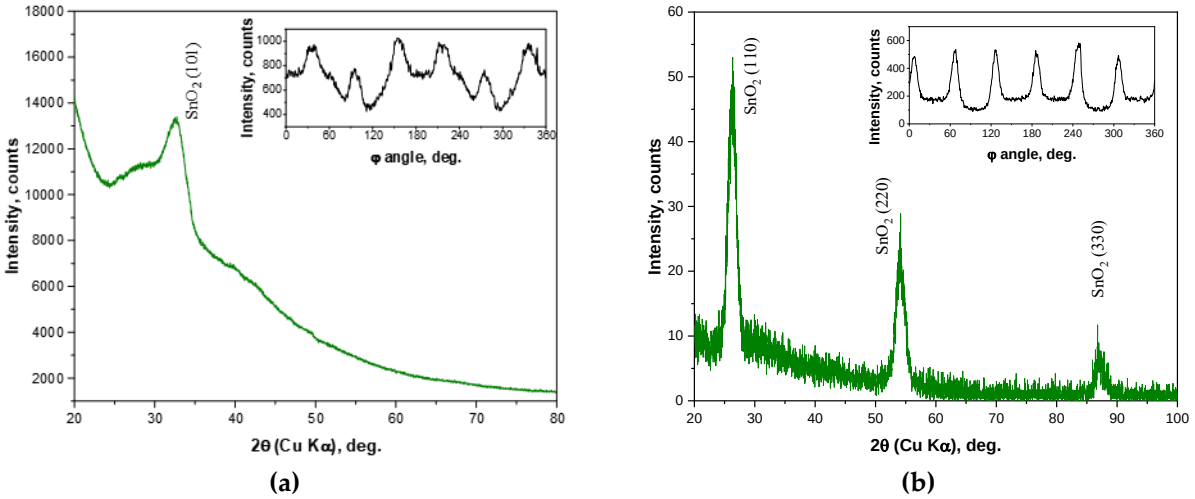

Figure S2. The θ-2θ scan for **CoSO-1 sample (room temperature implantation)** under fixed tilt angles of: (**a**) – ψ = 56.2° and φ = 335°, (**b**) – ψ = 45° and φ = 126°. The inset in (**a**) shows the φ-scan of the (101) reflex under 2θ = 33.8° and ψ = 56.2°; in (**b**) – the φ-scan of the (110) reflex under 2θ = 26.6° and ψ = 45°.

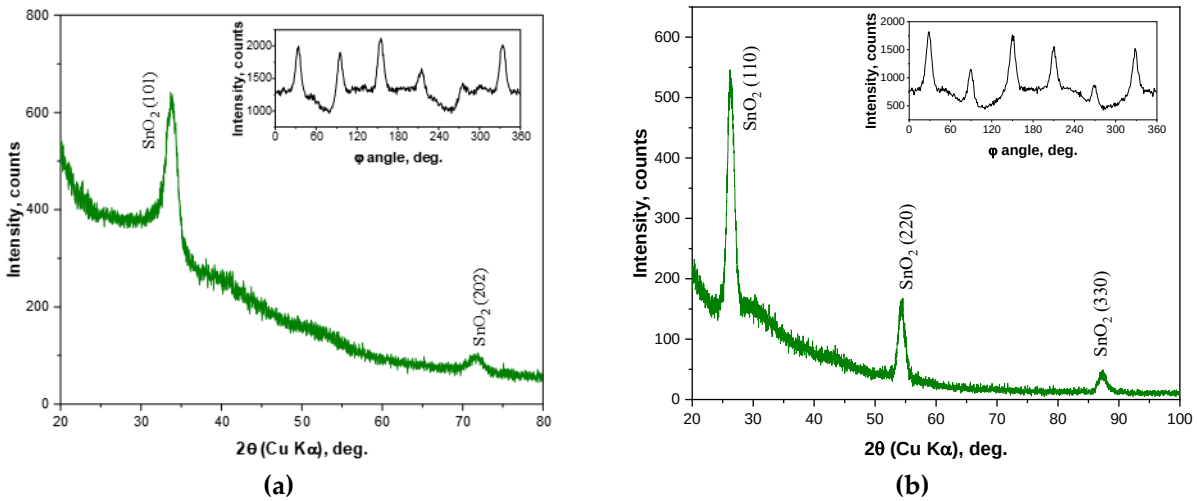

Figure S3. The θ-2θ scan for **CoSO-2h sample ("hot" implantation)** under fixed tilt angles of: (**a**) – ψ = 56.2° and φ = 335°, (**b**) – ψ = 45° and φ = 126°. The inset in (**a**) shows the φ-scan of the (101) reflex under 2θ = 33.8° and ψ = 56.2°; in (**b**) – the φ-scan of the (101) reflex under 2θ = 26.6° and ψ = 45°.

2. SEM study of both as-prepared and Co- (or Ar)-ions implanted SnO_2 films

The surface morphology and chemical element composition of SnO_2 samples were investigated utilizing an EVO 50 XVP scanning electron microscope (SEM) equipped with an energy dispersive X-ray (EDX) spectrometer (Oxford, Inca Energy 350). The SEM analysis of both the as-prepared and Co-ions implanted SnO_2 film is presented in **Figures S4**. The SEM images clearly illustrate that the surface of the SnO_2 films, upon intense ion irradiation, exhibits pronounced roughness along with the presence of blisters and neoplasms. The EDX spectrum confirms successful implantation of Co ions into the SnO_2 structure, and the EDX mapping reveals a homogeneous distribution of the cobalt implant at the submicron scale across the entire surface of the implanted SnO_2.

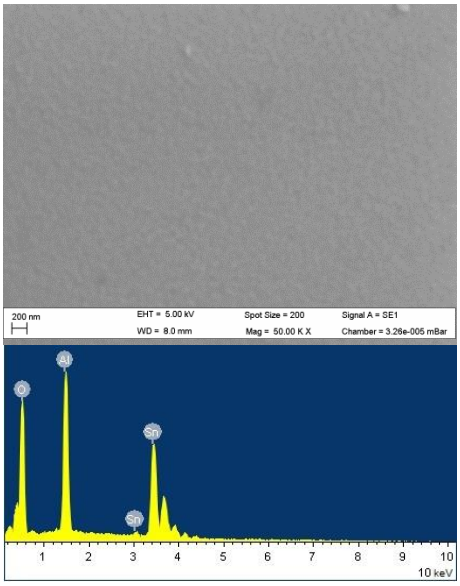

(a)

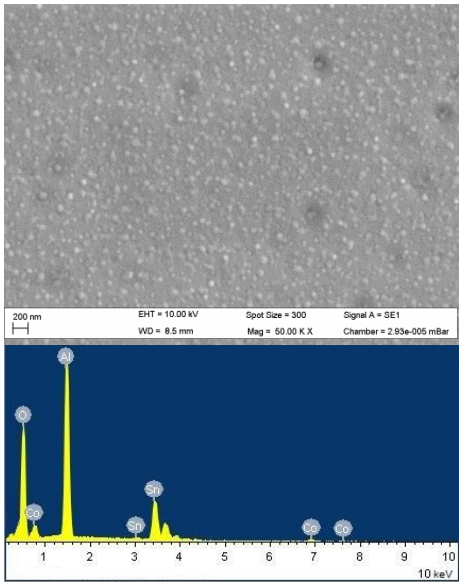

(b)

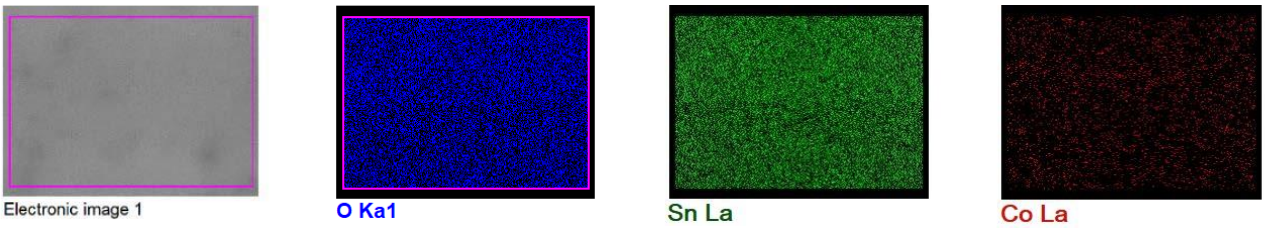

(c)

Figure S4. SEM images of the surface of SnO_2 film before **(a)** and after **(b)** implantation with 40 keV Co+ ions to the fluence of 1.0×10^{17} ion/cm^2; **(c)** –EDX elemental mapping of the surface of the Co-ions implanted SnO_2 film at the submicron (20,000x magnification) scale.

The similar picture is taken place in Ar-ions implanted SnO_2 film (see **Figure S5**). Here, the neoplasms with semi-spherical form are also observed on the surface of the film after intense irradiation with argon ions, but their surface density is lower than the density of new formations in films implanted with cobalt ions. Since the EDX spectrum of Ar-ions implanted SnO2 film (not shown) reveals very week energy peaks associated with argon, we can conclude that the most of chemically inert argon leaves the implanted SnO_2 film due to outward diffusion process.

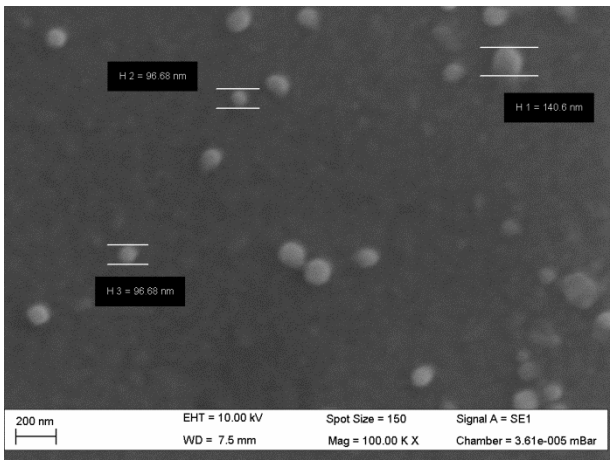

(a)

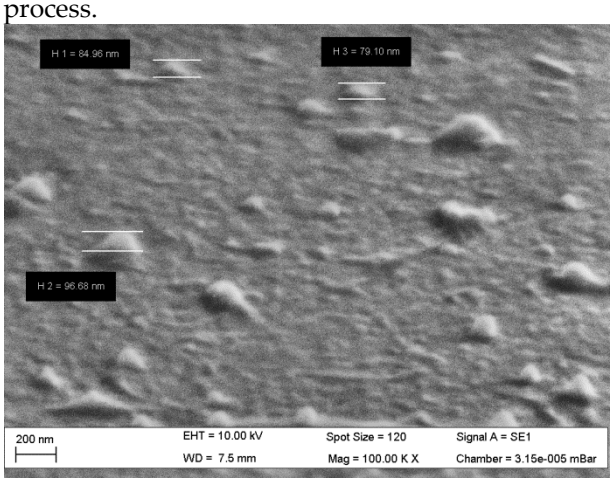

(b)

Figure S5. SEM image of the surface of SnO_2 film after implantation with 40 keV Ar+ ions to the fluence of 1.0×10^{17} ion/cm^2 **(a)** and SEM image of same film under 70° degrees with respect to electron beam **(b)**.

3. AFM study of both as-prepared and Co-ions implanted SnO_2 films

Atomic force microscopy (AFM) study of the surface morphology of SnO_2 films was performed in additional to SEM study. The Dimension FastScan Bruker AFM has been used for this purpose. An AFM study of the surface morphology of as-prepared SnO_2 films (**Figure S6a**) showed that film surface is quite smooth with a roughness of 5-7 nm. On the contrary, AFM image presented in **Figure S6b** show that large neoplasms (~40-70 nm in sizes) are formed on the surface of the film after high-fluence implantation with Co ions.

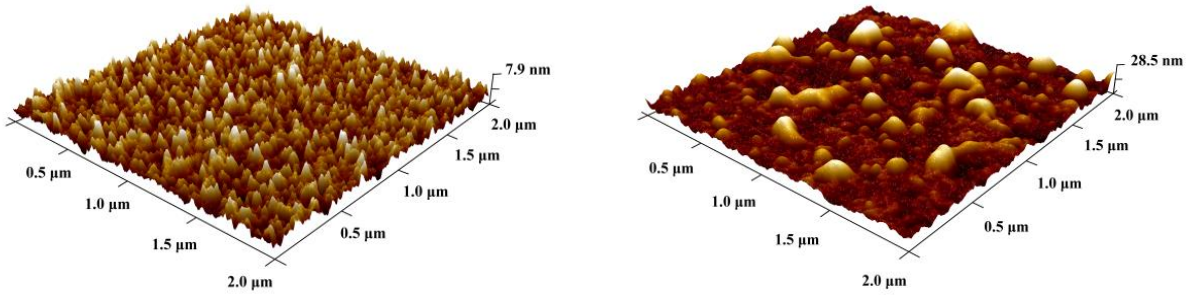

(a) (b)

Figure S6. AFM images of the surface of SnO_2 film before **(a)** and after **(b)** implantation with 40 keV Co+ ions to the fluence of 1.0×10^{17} ion/cm^2.

4.119. Sn Mössbauer studies of the epitaxial SnO_2 film on C-cut Al_2O_3 substrate before and after Co ions implantation

Room-temperature transmission ^{119}Sn Mössbauer studies were carried out using conventional WissEl spectrometer working in the constant acceleration mode. ^{119m}Sn($CaSnO_3$) source with an activity of about 15 mCi (RITVERC) was used. The spectrometer velocity scale was calibrated using thin metallic iron foil at room temperature. The spectra were least-squares fitted using SpectrRelax 2.1 software. The values of isomer shifts are determined versus center of polycrystalline thin SnO_2 absorber spectrum at room temperature.

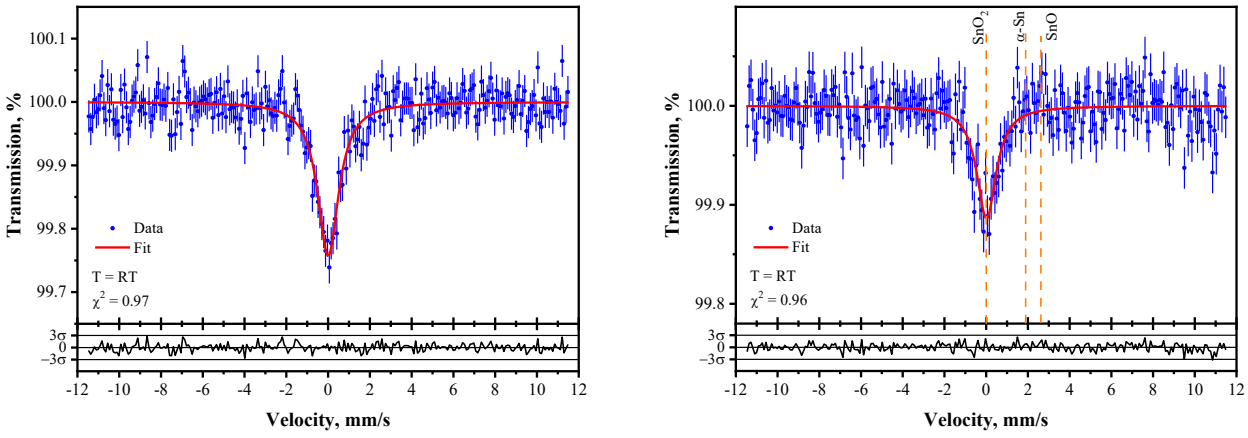

Figure S7. ^{119}Sn Mössbauer spectra of the epitaxial SnO_2 film on C-cut Al_2O_3 substrate before (**a**) and after (**b**) the implantation with 40 keV Co^+ ions with the fluence of 1×10^{17} ions/cm^2. Blue points with statistical error bars represent the experimental spectra, whereas solid red curves – the best-fit results. In panel (**b**) the dashed orange lines show

the isomer shift values for tin dioxide (SnO_2), tin monoxide (SnO) α-phase of metallic tin (α-Sn), respectively.

The results of ^{119}Sn Mössbauer studies of the epitaxial SnO_2 film on C-cut Al_2O_3 substrate before implantation is shown in **Figure S7(a)**. The spectrum of the film in the initial state was the single absorption line with the isomer shift corresponding to the Sn^{4+} ions in SnO_2. After Co ions implantation, the spectrum did not change qualitatively (**Figure S7(b)**). It should be noted that within the experimental signal-to-noise ratio the additional components corresponding to the tin ions in other states were not observed. It proves that the Co ions implantation did not notably affect the valence state of tin atoms in the implanted SnO_2 film. Moreover, there are no clear signs of the line broadening after the Co ions implantation. It was related with the fact the content of the atoms with the strong distorted local surrounding is small within the whole SnO_2 film.

5. High-resolution X-ray photoelectron spectra (XPS)

High-resolution XPS spectra were taken at room temperature by using a Phoibos 150 hemispherical energy analyzer (SPECS GmbH, Berlin, Germany). The obtained results were analyzed using CasaXPS software. The experimental data both for as-prepared SnO_2 films and Co-ions implanted CoSO-1 sample are depicted in **Figure S8.** It was established that the valence states of tin and oxygen atoms are preserved under the Co ions implantation and the XPS peak positions correspond to Sn^{4+} and O^{2-} states. At the same time, Co implant was found in the mixed valence state: either in the form of metal atom Co^0 or Co^{2+} ions. The detailed deconvolution of Co2$p_{3/2}$ region into components is presented in the paper.

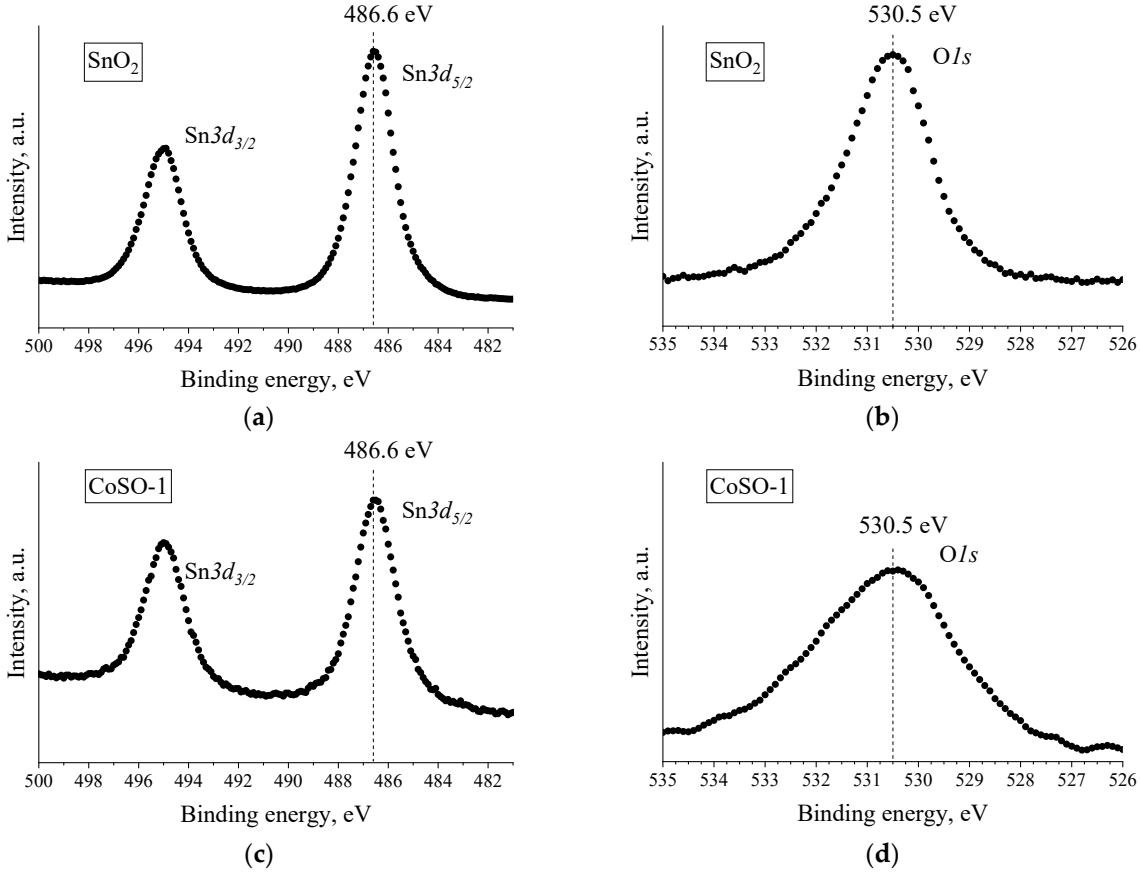

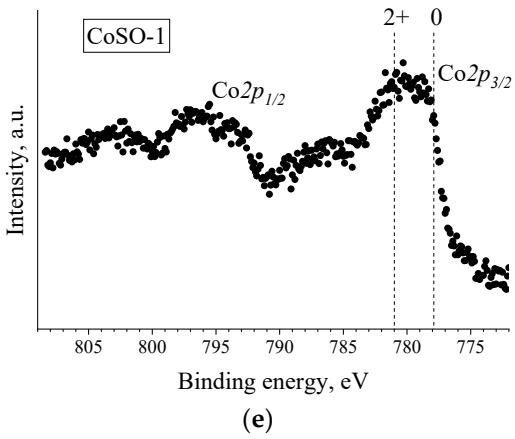

Figure S8. High-resolution XPS spectra of Sn3*d* (**a, c**), O1*s* (**b, d**) and Co2*p* (**e**) in both as-prepared SnO_2 film (**a, b**) and CoSO-1 sample implanted with 40 keV Co^+ ions to the fluence of 1×10^{17} ions/cm^2 at room substrate temperature (**c, d, e**).

6. Magnetic properties of undoped epitaxial SnO_2 films

Figure S9 show the magnetization curves recorded *in-plane* geometry for as-prepared epitaxial SnO_2 film with thickness of 140 nm (black curve), as well for the same films after vacuum annealing (red curve) or after Ar-ions high-fluence implantation (blue curve). It is clearly seen that in the epitaxial SnO_2 film reveals diamagnetic behavior at room temperature. The subsequent annealing of SnO_2 film in a high vacuum of 10^{-6} mmHg at temperature of 873 K for 30 minutes, as well as the implantation with 40 keV inert Ar ions to the fluence of 1.0×10^{17} ion/cm^2 at ion flux of 2-3 μA/cm^2 induce paramagnetic response in SnO_2 film. The observed paramagnetism may be related to the formation of paramagnetic point defects (tin or oxygen vacancies) in the bulk of the annealed or Ar-ions implanted SnO_2 films.

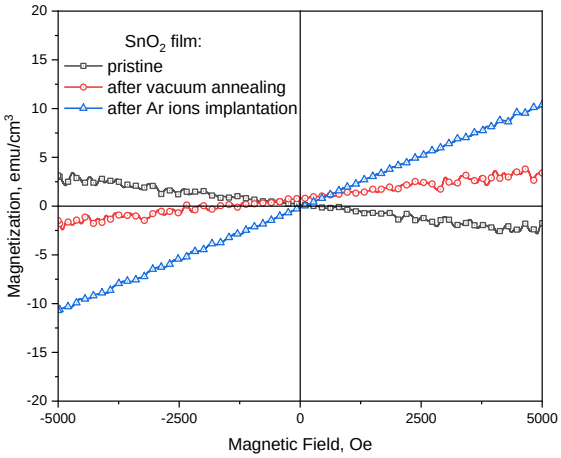

Figure S9. The room temperature magnetization curves of SnO_2 films in the pristine state (black curve), after annealing in high vacuum (red curve), and after 40 keV Ar^+ ions implantation to the fluence of 1×10^{17} ions/cm^2 (blue curve). Diamagnetic contribution of Al_2O_3 substrate was subtracted.

7. Easy-plane magnetic anisotropy in Co-ions implanted SnO_2 films

Figure S10 shows the magnetic hysteresis loops of CoSO-1 and CoSO-2h samples recorded at room temperature with magnetic field sweep up to 5 kOe either in sample plane (in-plane geometry) or along to the normal of sample plane (out-of-plane geometry). It is important to note that the diamagnetic contribution of the Al_2O_3 substrate was subtracted from magnetic measurements, and the value of the measured magnetic moment was normalized to the area of specimens under study in order to calculate the magnetization per implanted cobalt atom.

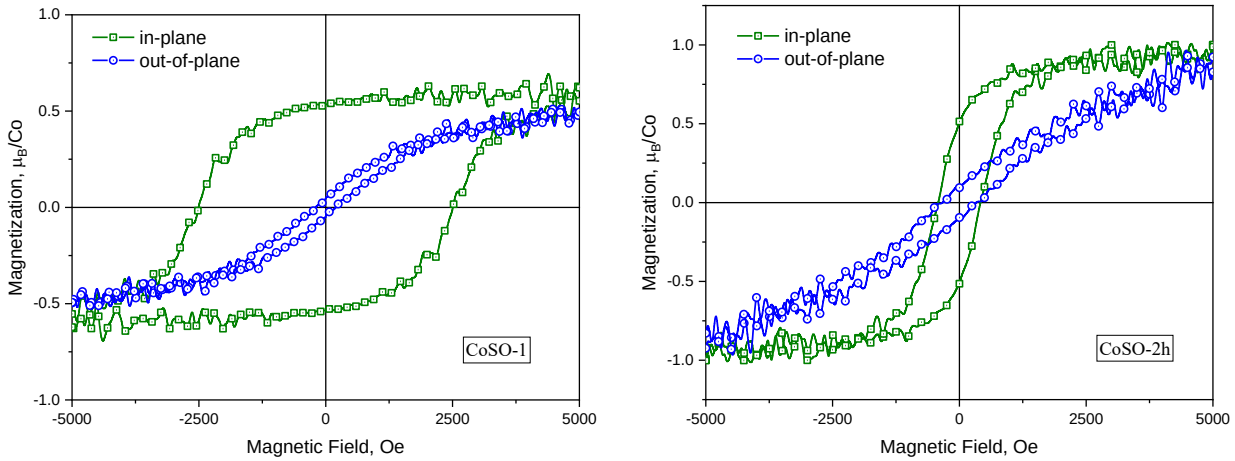

(**a**) (**b**)

Figure S10. The room temperature magnetic hysteresis loops recorded in the in-plane (green) and out-of-plane (blue) geometries of magnetic field sweep for CoSO-1 (**a**) and CoSO-2h (**b**) samples.